Research on integrated controller to reduce the roll and pitch of the AUV with horizontal rudder

Qi Zhigang[a], Hui Jiuwu[a*], Yuan Xin[a], Philip Wilson[b]

a College of Automation, Harbin Engineering University, Harbin 150001, China

b Fluid-Structure Interactions Research Group, School of Engineering Sciences

University of Southampton, Southampton, United Kingdom

E-mail address: huijiuwu123@163.com (H. Jiuwu), qzggo@163.com (Q. Zhigang)

Abstract

When underwater vehicles sail near the surface at low speed, they will experience roll, pitch and heave heavily due to the disturbance from waves, sea wind, and currents. In order to improve the ability of the underwater vehicle to resist the disturbance, the horizontal rudder using the lift principle of zero speed fin stabilizer is proposed to reduce the roll and pitch of the underwater vehicle. Considering the underwater vehicle's 6-DOF nonlinear and coupling motions and the working principle of the horizontal rudder, a modified sliding mode integrated controller is designed to reduce the roll and pitch under different wave disturbances. After analyzing the simulation results, it shows that the control law can reduce the roll and pitch of an underwater vehicle effectively.

Keywords: AUV anti roll; AUV anti pitch; horizontal rudder; sliding mode integrated controller

1.Introduction

An autonomous underwater vehicle(AUV) is a submersible vehicle, which can

navigate, control and accomplish the tasks under different ocean environments all autonomously (Yan and Zhou, 2015). With the development of ocean engineering, many countries are studying new types of underwater vehicles to carry out different types of missions in complex ocean environments. Underwater vehicles will experience roll, pitch and heave heavily when they close to the surface where there are much influence from waves, sea wind, currents and submarine topography etc (Qi et al., 2011; Qi et al., 2011). These disturbances seriously influence the normal working and safety of the underwater vehicle. Many researchers had simulated and analyzed 6-DOF motions of the underwater vehicle (Fang et al., 2006; Mills and Harris, 1995; Petrich and Stilwell, 2010), however, the simulation results show that their control methods could hardly solve the roll and pitch motion control problem very well.

The use of a fin stabilizer is one of the most effective roll stabilization equipment. The horizontal rudder based on the working principle of the zero speed fin stabilizer can realize active roll and pitch stabilization at low speed or at anchor. When the underwater vehicle navigates at medium or high speed, the operating principle of the horizontal rudder is the same as the fin stabilizer, the horizontal rudder keeps a fixed attack angle to generate the desired lift. When the underwater vehicle navigates at low speed or at anchor, the horizontal rudder can produce the designed lift by flapping around the axis actively (Fan et al., 2009). The shape of the horizontal rudder is different from the common fin stabilizer, it has low aspect ratio and the position of the horizontal rudder is closer to the leading edge and trailing edge of underwater vehicle. The low aspect ratio can increase the time the vortex is attached to the rudder surface, hence it can increase the rudders flapping lift. The fluid resistance of the horizontal rudder includes shape drag, added mass force and vortex inducting force (Fan et al.,

2009; Jin et al., 2007; Qi., 2008).

Nowadays, sliding mode control method is widely applied in nonlinear time-varying systems, such as Cui et al. (2016); Jantapremjit and Wilson (2007); Hao and Zhao (2013); Jafarov and Asaltin (2000); Rhif et al. (2011) and Jantapremjit et al. (2006). Considering the underwater vehicle's 6-DOF nonlinear and coupling motions and the working principle of the horizontal rudder, a modified sliding mode integrated controller is designed to reduce the roll and pitch under different wave disturbances.

In this paper, a method to reduce the roll and pitch is presented by using the horizontal rudder of the AUV based on the operating principle of the zero speed fin stabilizer. A modified sliding mode control is proposed based on the 6-DOF motions of underwater vehicle and the operating principle of horizontal rudder. Finally, simulations were presented to verify the validity of the control law proposed.

2.The model of underwater vehicle

In this paper, NPS AUV II is considered as a research model. NPS AUV II is manufactured by Naval Postgraduate School (NPS) of America in 1987. It is used as basic research platform including control technology, artificial intelligence and system synthesis (Warner, 1991; Healey and Marco, 1992). NPS AUV II is shown in Fig. 1, which has a pair of bowplanes are shown as 2, 3, and a pair of sternplanes are shown as 1, 4. In this paper, the bowplanes and sternplanes are regarded as horizontal rudders which use the lift principle of zero speed fin stabilizer to generate hydrodynamic force to stabilize the underwater vehicle.

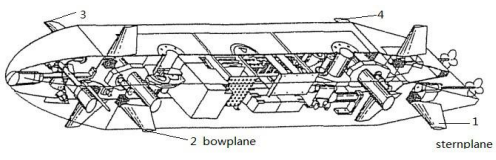

Fig. 1 Schematic diagram of the NPS AUV II

The 6-DOF nonlinear motion equations are presented in Fossen (1994).

Surge motion equation

$$
\begin{aligned}
&m[\dot{u} - vr + wq - x_G(q^2 + r^2) + y_G(pq - \dot{r}) + z_G(pr + \dot{r}) \\
&= \frac{\rho}{2}L^4\left[X'_{pp}p^2 + X'_{qq}q^2 + X'_{rr}r^2 + X'_{pr}pr\right] + \frac{\rho}{2}L^3[X'_{\dot{u}}\dot{u} + X'_{wq}wq + X'_{vp}vp + X'_{vr}vr + \\
&uq\left(X'_{q\delta_s}\delta_s + X'_{q\delta_{bp}}\delta_{bp} + X'_{q\delta_{bs}}\delta_{bs}\right) + X'_{r\delta_r}ur\delta_r] + \frac{\rho}{2}L^2[X'_{vv}v^2 + X'_{ww}w^2 + X'_{v\delta_r}\delta_r + \\
&uw\left(X'_{w\delta_s}\delta_s + X'_{w\delta_{bs}}\delta_{bs} + X'_{w\delta_{bp}}\delta_{bp}\right) + u^2\left(X'_{\delta_s\delta_s}\delta_s^2 + X'_{\delta_{bp}\delta_{bp}}\delta_{bp}^2 + X'_{\delta_r\delta_r}\delta_r^2\right) - (W - B)\sin\theta + \\
&\frac{\rho}{2}L^3X'_{q\delta_{sn}}uq\delta_s\varepsilon(n) + \frac{\rho}{2}L^2\left(X'_{w\delta_{sn}}uw\delta_{sn} + X'_{\delta_s\delta_{sn}}u^2\delta_s^2\right)\varepsilon(n) + \frac{\rho}{2}L^2u^2X'_{prop} \\
&+ F_{yz}
\end{aligned}
$$

Sway motion equation

$$
\begin{aligned}
&m[\dot{v} + ur - wp + x_G(pq + r^2) - y_G(p^2 + r^2) + z_G(qr - \dot{p}) \\
&= \frac{\rho}{2}L^4\left[Y'_{\dot{p}}\dot{p} + Y'_{\dot{r}}\dot{r} + Y'_{pq}pq + Y'_{qr}qr\right] + \frac{\rho}{2}L^3[Y'_{\dot{v}}\dot{v} + Y'_{P}up + X'_{r}ur + Y'_{vq}vq + Y'_{wp}wp + Y'_{wr}wr] \\
&+ \frac{\rho}{2}L^2[Y'_{v}uv + Y'_{vw}uw + Y'_{\delta r}u^2\delta_r] - \frac{\rho}{2}\int_{x_{tail}}^{x_{nose}}[C_{dy}h(x)(v + xr)^2 + C_{dz}b(x)(w - xq)^2]\frac{(v + xr)}{U_{cf}(x)}dx \\
&+ (W - B)\cos\theta\sin\phi \\
&+ F_{xz}
\end{aligned}
$$

Heave motion equation

$$
\begin{aligned}
&m[\dot{w} - uq + vp + x_G(pr - \dot{q}) + y_G(qr + \dot{p}) - z_G(p^2 + q^2) \\
&= \frac{\rho}{2}L^4\left[Z'_{\dot{q}}\dot{q} + X'_{pp}p^2 + X'_{pr}pr + X'_{rr}r^2\right] + \frac{\rho}{2}L^3[Z'_{\dot{w}}\dot{w} + Z'_{q}uq + Z'_{vp}vp + Z'_{vr}vr] \\
&+ \frac{\rho}{2}L^2[Z'_{w}uw + Z'_{vv}v^2 + u^2\left(Z'_{\delta_s}\delta_s + Z'_{\delta_{bs}}\delta_{bs} + Z'_{\delta_{bp}}\delta_{bp}\right)] + \\
&\frac{\rho}{2}\int_{x_{tail}}^{x_{nose}}\left[C_{dy}h(x)(v + xr)^2 + C_{dz}b(x)(w - xq)^2\right]\frac{(w - xq)}{U_{cf}(x)}dx + \\
&(W - B)\cos\theta\cos\phi + \frac{\rho}{2}L^3Z'_{qn}uq\varepsilon(n) + \frac{\rho}{2}L^2\left(Z'_{wN}uw + Z'_{\delta\delta_{sn}}u^2\delta_s^2\right)\varepsilon(n) \\
&+ F_{xy}
\end{aligned}
$$

Roll motion equation

$$
\begin{aligned}
&I_x\dot{p} + (I_z - I_y)qr + I_{xy}(pr - \dot{q}) - I_{yz}(q^2 - r^2) - I_{xz}(pq + \dot{r}) \\
&+ m[y_G(\dot{w} - uq + vp) - z_G(\dot{v} + ur - wp)] \\
&= \frac{\rho}{2}L^5[K'_{\dot{p}}\dot{p} + K'_{\dot{r}}\dot{r} + K'_{pq}pq + K'_{qr}qr] + \\
&\frac{\rho}{2}L^4[K'_{\dot{v}}\dot{v} + K'_{p}up + K'_{r}ur + K'_{vq}vq + K'_{wp}wp + K'_{wr}wr] + \\
&\frac{\rho}{2}L^3[K'_{v}uv + K'_{vw}vw + u^2(K'_{\frac{\delta b}{2}}\delta_{bp} + K'_{\frac{\delta b}{2}}\delta_{bs})] + \\
&(y_GW - y_BB)\cos\theta\cos\phi - (z_GW - z_BB)\cos\theta\sin\phi + \\
&\frac{\rho}{2}L^4K'_{pn}up\varepsilon(n) + \frac{\rho}{2}L^3u^3K'_{prop} \\
&+ M_x
\end{aligned}
$$

Pitch motion equation

$$I_y \dot{q} + (I_x - I_z)pr - I_{xy}\left(qr + \dot{p}\right) + I_{yz}\left(pq - \dot{r}\right) + I_{xz}(p^2 - r^2)$$

$$- m[x_G(\dot{w} - uq + vp) - z_G(\dot{u} - vr + wq)]$$

$$= \frac{\rho}{2} L^5 [M'_{\dot{q}} \dot{q} + M'_{pp} p^2 + M'_{pr} pr + M'_{rr} r^2] +$$

$$\frac{\rho}{2} L^4 [M'_{\dot{w}} \dot{w} + M'_{uq} uq + M'_{vp} vp + M'_{vr} vr] +$$

$$\frac{\rho}{2} L^3 [M'_{uw} uw + M'_{vv} v^2 + u^2 (M'_{\delta_s} \delta_s + M'_{\frac{\delta b}{2}} \delta_{bp} + M'_{\frac{\delta b}{2}} \delta_{bs})] -$$

$$\frac{\rho}{2} \int_{x_{tail}}^{x_{nose}} [C_{dy} h(x)(v + xr)^2 + C_{dz} b(x)(w - xq)^2] \frac{(w + xq)}{U_{cf}(x)} x dx -$$

$$(x_G W - x_B B)\cos\theta\cos\phi - (z_G W - z_B B)\sin\theta +$$

$$\frac{\rho}{2} L^4 M_{pn} up\varepsilon(n) + \frac{\rho}{2} L^3 [M'_{wn} uw + M'_{\delta n} u^2 \delta_s]\varepsilon(n)$$

$$+ M_y$$

Yaw motion equation

$$I_z \dot{r} + (I_y - I_x)pq - I_{xy}(p^2 - r^2) - I_{yz}\left(pr + \dot{q}\right) + I_{xz}\left(qr - \dot{p}\right)$$

$$+ m[x_G(\dot{v} + ur - wp) - z_G(\dot{u} - vr + wq)]$$

$$= \frac{\rho}{2} L^5 [N'_{\dot{p}} \dot{p} + N'_{\dot{r}} \dot{r} + N'_{pq} pq + N'_{qr} qr] +$$

$$\frac{\rho}{2} L^4 [N'_{\dot{v}} \dot{v} + N'_{p} up + M'_{r} ur + M'_{vq} vq + M'_{wp} wp + M'_{wr} wr] +$$

$$\frac{\rho}{2} L^3 [N'_{v} uv + N'_{vw} vw + N'_{\delta r} u^2 \delta_r] -$$

$$\frac{\rho}{2} \int_{x_{tail}}^{x_{nose}} [C_{dy} h(x)(v + xr)^2 + C_{dz} b(x)(w - xq)^2] \frac{(v + xr)}{U_{cf}(x)} x dx +$$

$$(x_G W - x_B B)\cos\theta\sin\phi + (y_G W - y_B B)\sin\theta + \frac{\rho}{2} L^3 u^2 N'_{prop}$$

$$+ M_z$$

Where m is the mass of underwater vehicle; u, v, and w represent surge, sway and heave velocity, respectively; p, q, and r represent roll, pitch, and yaw angular velocity, respectively; ∂_s, ∂_b, and ∂_r represent bowplane, sternplane, and rudder angle, respectively; ϕ, θ, and ψ represent roll, pitch, and yaw angle, respectively; L is the total length of AUV; m is the mass of AUV; I_x, I_y, I_z are the moments of inertia about the X, Y, and Z-axis; x_G, y_G, z_G are the coordinate of the center of gravity;

$I_{xy} = I_{yx}$, $I_{xz} = I_{zx}$, $I_{yz} = I_{zy}$ are the products of inertia; F_{yz}, F_{xy}, F_{xz} are the forces of waves about the X, Y, and Z-axis; M_x, M_y, M_Z are the moments of waves about the X, Y, and Z-axis; and other parameters are relevant hydrodynamics coefficients which are recommended by ITTC (International Towing Tank Conference).

The above nonlinear equations are deduced by applying the Newtonian second law and hydromechanics theory based on the underwater vehicle which is regarded as a rigid body with a uniform mass distribution. These equations are the basis of researching 6-DOF motions of the underwater vehicle. However these equations have many hydrodynamic coefficients and every freedom degree is coupled with others. In order to simplify the complexity of the simulation, we make following assumptions:

(1) The ideal movement of the underwater vehicle is that it keeps a constant surge velocity and constant depth in the ocean space, the sway and heave velocity and acceleration are zero, the roll, pitch and yaw angular velocity and angular acceleration are zero.

(2) The coupling effect between the roll motion, sway motion and yaw motion of underwater vehicle is stronger, and the coupling effect between the heave motion and pitch motion is also stronger. Hence the influence which the vertical plane motion exerts to the horizontal plane motion can be omitted and are therefore decoupled.

(3) In motion equations, retaining most of hydrodynamic coefficients that play the leading role of AUV and omitting others.

Based on the assumptions, the 6-DOF motion equations are simplified and shown as matrix form are as follows:

133 Surge motion equation

134 $$U \approx U_0 \tag{1}$$

135 Horizontal plane motion

136 $$\begin{bmatrix} a_{11} & a_{12} & a_{13} \\ a_{21} & a_{22} & a_{23} \\ a_{31} & a_{32} & a_{33} \end{bmatrix} \begin{bmatrix} \dot{v} \\ \dot{p} \\ \dot{r} \end{bmatrix} = u \begin{bmatrix} b_{11} & b_{12} & b_{13} \\ b_{21} & b_{22} & b_{23} \\ b_{31} & b_{32} & b_{33} \end{bmatrix} \begin{bmatrix} v \\ p \\ r \end{bmatrix} + \begin{bmatrix} F_{wxz} \\ M_{fin1} + M_{wx} \\ M_{wz} \end{bmatrix} \tag{2}$$

137 Where,

138 $$a_{11} = m - \frac{\rho}{2} L^3 Y'_{\dot{v}}, \quad a_{12} = -(mz_G + \frac{\rho}{2} L^4 Y'_{\dot{p}}), \quad a_{13} = -\frac{\rho}{2} L^4 Y'_{\dot{r}}, \quad a_{21} = -(mz_G + \frac{\rho}{2} L^4 K'_{\dot{v}}),$$

139 $$a_{22} = I_x - \frac{\rho}{2} L^5 K'_{\dot{p}}, \quad a_{23} = -\frac{\rho}{2} L^5 K'_{\dot{r}}, \quad a_{31} = -\frac{\rho}{2} L^4 N'_{\dot{v}}, \quad a_{32} = -(I_x + \frac{\rho}{2} L^5 N'_{\dot{p}}),$$

140 $$a_{33} = I_z + \frac{\rho}{2} L^5 N'_{\dot{r}}, \quad b_{11} = \frac{\rho}{2} L^2 Y'_v, \quad b_{12} = \frac{\rho}{2} L^3 Y'_p, \quad b_{13} = \frac{\rho}{2} L^3 Y'_r - m, \quad b_{21} = \frac{\rho}{2} L^3 K'_v,$$

141 $$b_{22} = \frac{\rho}{2} L^4 K'_p, \quad b_{23} = \frac{\rho}{2} L^4 K'_r + mz_G, \quad b_{31} = \frac{\rho}{2} L^3 N'_v, \quad b_{32} = \frac{\rho}{2} L^4 N'_p, \quad b_{33} = \frac{\rho}{2} L^4 N'_r.$$

142 Vertical plane motion

143 $$\begin{bmatrix} c_{11} & c_{12} \\ c_{21} & c_{22} \end{bmatrix} \begin{bmatrix} \dot{w} \\ \dot{q} \end{bmatrix} = u \begin{bmatrix} d_{11} & d_{12} \\ d_{21} & d_{22} \end{bmatrix} \begin{bmatrix} w \\ q \end{bmatrix} + \begin{bmatrix} F_{wxy} \\ M_{fin2} + M_{wy} \end{bmatrix} \tag{3}$$

144 Where,

145 $$c_{11} = m - \frac{\rho}{2} L^3 Z'_{\dot{w}}, c_{12} = \frac{\rho}{2} L^4 Z'_{\dot{q}}, c_{21} = -\frac{\rho}{2} L^4 M'_{\dot{w}}, c_{22} = I_y - \frac{\rho}{2} L^5 M'_{\dot{q}}, d_{11} = \frac{\rho}{2} L^2 Z'_w, d_{12} = \frac{\rho}{2} L^3 Z'_q,$$
$$d_{21} = \frac{\rho}{2} L^3 M'_{uw}, d_{22} = \frac{\rho}{2} L^4 M'_{uq}$$

146 The simplified 6-DOF motion equations can not only guarantee motions of the
147 underwater vehicle which are accurate and reasonable, but also make the simulation
148 easier.

3.The wave force and the moment of the AUV near the surface

The wave is regarded as a kind of stationary random process. In order to perform the simulation, the long-crested wave are used to simulate the environment disturbance and high order harmonics of waves is neglected. Long-crested waves are expressed as follows (Jin and Yao, 2011):

$$\zeta(t)=\sum_{i=1}^{\infty}\zeta_{ai}\cos(\omega_i t+\varepsilon_i) \tag{4}$$

Where ζ is the wave amplitude; ω_i is the wave frequency; phase ε_i is a random variable, which is a kind of uniform during $0\sim 2\pi$.

According to hydrodynamic theory, wave motion is a circular motion which is formed by the uniform motion of water particles along the circular orbit. The relationship between the circular motion radii ς_B and the water depth h_B is expressed as follows:

$$\varsigma_B=\varsigma_A e^{-\frac{2\pi h_B}{\lambda}}=\varsigma_A e^{-h_B k} \tag{5}$$

The long-crested wave in the depth h_B is expressed as follows:

$$\zeta_w=\sum_{i=1}^{n}e^{-h_B k_i}\zeta_{ai}\cos\left(\omega_i t+\varepsilon_i\right) \tag{6}$$

Based on the above expression, the any point velocity and acceleration of sea waves is expressed as follows:

$$\begin{aligned} V_W&=\frac{d\zeta_W}{dt}=-\omega_i\sum_{i=1}^{n}e^{-h_B k_i}\zeta_i\sin(\omega_i t+\varepsilon_i)\\ a_W&=\frac{dV_W}{dt}=-\omega_i^{\,2}\sum_{i=1}^{n}e^{-h_B k_i}\zeta_i\cos(\omega_i t+\varepsilon_i)\end{aligned} \tag{7}$$

In this paper, the simulation is based on ITTC two-parameter ocean wave spectrum. The ITTC two-parameter wave spectrum is expressed as follows:

$$S_{\zeta}(\omega)=\frac{A}{\omega^5}\exp\left(-\frac{B}{\omega^4}\right) \tag{8}$$

Where $A=173*\frac{h^2_{1/3}}{T^4}, B=\frac{691}{T^4}$, $h_{1/3}$ is the significant wave height, T is the period of waves.

Forces and moments acting on the underwater vehicle includes: hydrodynamic forces and moments, forces and moments are generated by underwater vehicle's actuator, the gravity and buoyancy of the underwater vehicle, forces and moments are generated by waves, sea wind, and currents. In order to simplify the calculation of waves force and moment for the underwater vehicle, the shape of the AUV is simplified. It compose a cylinder in the middle and two hemispheres on the both end (Ji, 2009). Parameters of the simplified shape of the AUV include: the underwater vehicle's total length L is 5.3 m, radius R is 0.5m, and width B is 1m, the shape is shown as follows:

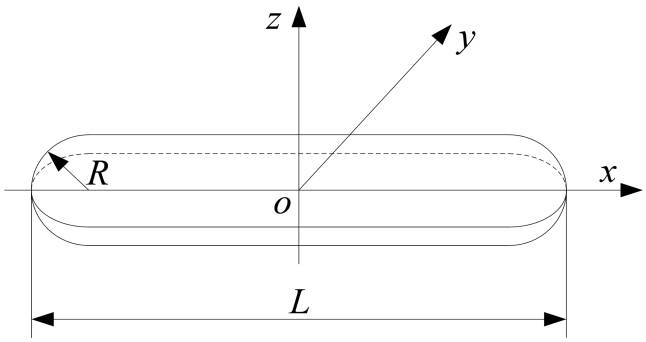

Fig.2 Simplified AUV AUV figure

The shape of the AUV is mathematical expressed as follows:

$$\begin{cases} \left(x+L/2-R\right)^2+y^2+z^2=R^2 & \left(-L/2\le x\le -L/2+R\right) \\ y^2+z^2=R^2 & \left(-L/2+R\le x\le L/2-R\right) \\ \left(x-L/2+R\right)^2+y^2+z^2=R^2 & \left(L/2-R\le x\le L/2\right) \end{cases} \tag{9}$$

The above expression can also be expressed as follows:

$$\left(z-z'\right)=\begin{cases} 2\sqrt{R^2-y^2-\left(x+L/2-R\right)^2} & \left(-L/2\le x\le -L/2+R\right) \\ 2\sqrt{R^2-y^2} & \left(-L/2+R\le x\le L/2-R\right) \\ 2\sqrt{R^2-y^2-\left(x-L/2+R\right)^2} & \left(L/2-R\le x\le L/2\right) \end{cases}$$

$$\left(y-y'\right)=\begin{cases} 2\sqrt{R^2-z^2-\left(x+L/2-R\right)^2} & \left(-L/2\le x\le -L/2+R\right) \\ 2\sqrt{R^2-z^2} & \left(-L/2+R\le x\le L/2-R\right) \\ 2\sqrt{R^2-z^2-\left(x-L/2+R\right)^2} & \left(L/2-R\le x\le L/2\right) \end{cases} \tag{10}$$

$$\left(x-x'\right)=\begin{cases} 2\sqrt{R^2-y^2-z^2}+2R-L & \left(-0.5\le y\le 0\right) \\ 2\sqrt{R^2-y^2-z^2}-2R+L & \left(0\le y\le 0.5\right) \end{cases}$$

According to hydrodynamic theory, the fluid resistance of the symmetrical object is expressed as follows:

$$F_f=C_D\rho\frac{\left(V_W-V_S\right)^2}{2}S \tag{11}$$

Where C_D is drag coefficient; ρ is fluid density; $V_w=d_{\zeta_w}/d_t$ is the fluid velocity without disturbance; $V_s=d_{\zeta_s}/d_t$ is the vertical velocity of object; S is the projection area of object perpendicular to V_W or V_s.

The fluid inertial force of the accelerating object in fluid is expressed as follows:

196 $$F_a = kM'(a_w - a_s) = kM'\left(\frac{d^2\zeta_W}{dt^2} - \frac{d^2\zeta_s}{dt^2}\right) \tag{12}$$

197 Where k is added mass coefficient; M' is discharged fluid mass by object; a_w is
198 the fluid acceleration without disturbed; a_s is the acceleration of the object in
199 resistance direction.

200 The vertical velocity and acceleration at any point (x, y, z) of AUV are expressed as
201 follows:

202 $$\begin{aligned} V &= V_S + \omega_x y - \omega_y x \\ a &= a_S + \varepsilon_x y - \varepsilon_y x \end{aligned} \tag{13}$$

203 Where V_s is the speed in the AUV centroid; ω_s is the roll angular velocity; ω_y is
204 the pitch angular velocity; a_s is the acceleration in the AUV centroid; ε_x is the roll
205 angular acceleration; ε_y is the pitch angular acceleration.

206 The velocity and acceleration at each point of the AUV is different, hence wave
207 forces and moments are calculated by the integral method. The results of the
208 calculation are as follows:

209 Heave force equation

210 $$dF_{xy} = C_D\rho\frac{(V_W - V)^2}{2}dxdy + (a_w - a)\rho(z - z')dxdy$$

211 $$= C_D\rho\frac{\left[-\omega_i\sum_{i=1}^{n} e^{-h_b k_i}\zeta_i \sin(\omega_i t + \varepsilon_i) - V\right]^2}{2}dxdy +$$

212 $$[-\omega_i^2\sum_{i=1}^{n} e^{-h_b k_i}\zeta_i \cos(\omega_i t + \varepsilon_i) - a]\rho(z - z')dxdy$$

213 Sway force equation

214 $$dF_{xz} = C_D \rho \frac{(V_W - V_h)^2}{2} dxdz + (a_w - a_h)\rho(y - y')dxdz$$

215 $$= C_D \rho \frac{\left[-\omega_i \sum_{i=1}^{n} e^{-h_b k_i} \zeta_i \sin(\omega_i t + \varepsilon_i) - V_h \right]^2}{2} dxdz +$$

216 $$[-\omega_i^2 \sum_{i=1}^{n} e^{-h_b k_i} \zeta_i \cos(\omega_i t + \varepsilon_i) - a_h]\rho(y - y')dxdz$$

217 Surge force equation

218 $$dF_{yz} = C_D \rho \frac{(V_W - V_h)^2}{2} dydz + 0.5(a_w - a_h)\rho(x - x')dydz$$

219 $$= C_D \rho \frac{\left[-\omega_i \sum_{i=1}^{n} e^{-h_b k_i} \zeta_i \sin(\omega_i t + \varepsilon_i) - V_h \right]^2}{2} dydz +$$

220 $$0.5[-\omega_i^2 \sum_{i=1}^{n} e^{-h_b k_i} \zeta_i \cos(\omega_i t + \varepsilon_i) - a_h]\rho(x - x')dydz$$

221 Roll moment equation

222 $$dM_x = C_D \rho \frac{(V_W - V)^2}{2} ydxdy + (a_w - a)\rho(z - z')ydxdy$$

223 $$= C_D \rho \frac{\left[-\omega_i \sum_{i=1}^{n} e^{-h_b k_i} \zeta_i \sin(\omega_i t + \varepsilon_i) - V \right]^2}{2} ydxdy +$$

224 $$[-\omega_i^2 \sum_{i=1}^{n} e^{-h_b k_i} \zeta_i \cos(\omega_i t + \varepsilon_i) - a]\rho(z - z')ydxdy$$

225 Pitch moment equation

226 $$dM_y = C_D\rho\frac{(V_W - V)^2}{2}xdxdy + 0.5(a_w - a)\rho(z - z')xdxdy$$

227 $$= C_D\rho\frac{\left[-\omega_i\sum_{i=1}^{n}e^{-h_b k_i}\zeta_i\sin(\omega_i t + \varepsilon_i) - V\right]^2}{2}xdxdy +$$

228 $$0.5[-\omega_i^2\sum_{i=1}^{n}e^{-h_b k_i}\zeta_i\cos(\omega_i t + \varepsilon_i) - a]\rho(z - z')xdxdy$$

229 Yaw moment equation

230 $$dM_z = C_D\rho\frac{(V_W - V)^2}{2}zdxdz + (a_w - a)\rho(y - y')zdxdz$$

231 $$= C_D\rho\frac{\left[-\omega_i\sum_{i=1}^{n}e^{-h_b k_i}\zeta_i\sin(\omega_i t + \varepsilon_i) - V\right]^2}{2}zdxdz +$$

232 $$[-\omega_i^2\sum_{i=1}^{n}e^{-h_b k_i}\zeta_i\cos(\omega_i t + \varepsilon_i) - a]\rho(y - y')zdxdz$$

233 After the detailed calculation, numerical equations of wave forces and moments
234 can be obtained.

235 **4.The hydrodynamic model of horizontal rudder**

236 In this paper, an integrated controller to reduce roll and pitch is designed with the
237 horizontal rudder based on the operating principle of zero speed fin stabilizer. The
238 shape of the horizontal rudder is different from the normal fin stabilizer, it has a low
239 aspect ratio and the position of horizontal rudder is closer to leading edge and trailing
240 edge of the underwater vehicle. The low aspect ratio can increase the time the vortex
241 is attached to the rudder surface, hence it can increase the rudders flapping lift. The
242 working principle and model of zero speed fin stabilizer is shown as follows:

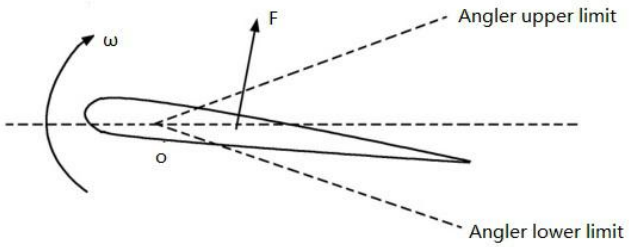

Fig. 3 Working principle of zero speed fin stabilizer

Jin et al. (2007) presented the resultant force of the horizontal rudder can be expressed as follows:

$$F(t)=\frac{e\rho}{3}\left(C_d+3k\right)\left(3a^2c+c^3\right)\omega^2(t)+\frac{J}{d}\dot{\omega}(t) \tag{14}$$

Where C_D is the drag coefficient; $2a$ is the chord length of the horizontal rudder; c is the distance between the midpoint and the shaft of rudder; e is the span length of the rudder; $\omega(t)$ is the rudder's angular velocity; J is the added moment of inertia; ρ is the density of the fluid; d is the distance between the added mass force and rudder shaft.

If:

$$a_1=\frac{e\rho}{3}\left(C_d+3k\right)\left(3a^2c+c^3\right) \tag{15}$$

$$a_2=\frac{J}{d} \tag{16}$$

Where the resultant force of the horizontal rudder can be expressed as follows:

$$F(t)=a_1\omega^2(t)+a_2\dot{\omega}(t) \tag{17}$$

When the angle between horizontal rudder and horizontal direction is $\alpha(t)$, the lift $L(t)$ in the vertical direction is expressed as：

$$L(t) = F(t)\cos(\alpha(t)) \tag{18}$$

The model of the AUV with the horizontal rudder as shown in Fig.4. Establishing the hull coordinate system and numbering the four horizontal rudder as fin1, fin2, fin3, and fin4.The X-axis is the roll axis, the Y-axis is the pitch axis and the Z-axis is the yaw axis.

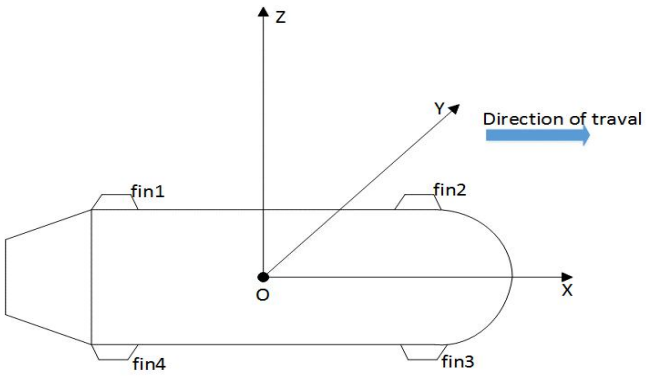

Fig.4 Schematic diagram of AUV with horizontal rudders

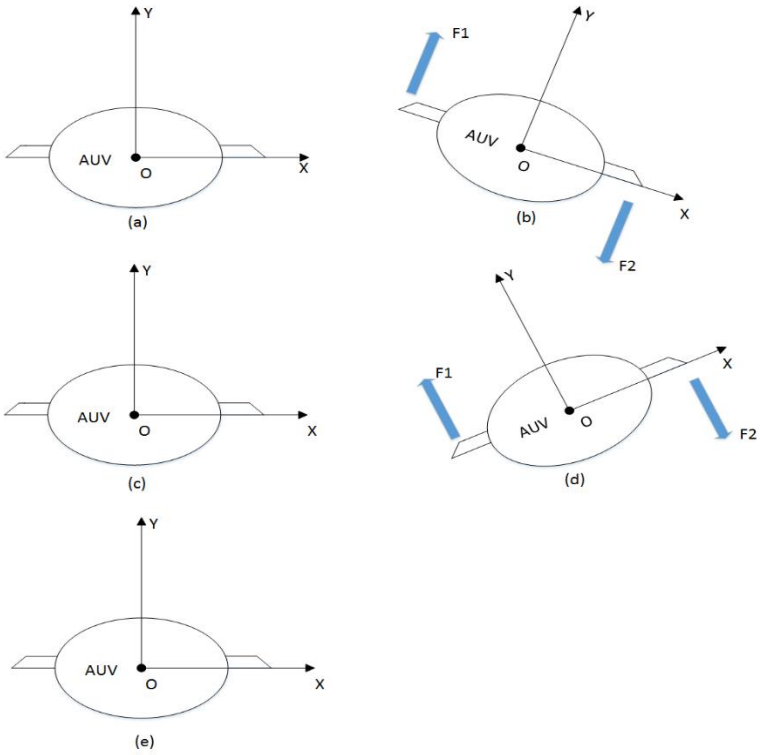

Fig.5 Working process of rolling motion reduction

The roll motion reduction process of the AUV is shown above. According to Fan et al. (2009); Jin et al. (2007) and Qi. (2008), when the underwater vehicle is in a calm ocean environment, the AUV can not generate roll motion as shown in Fig. 5(a), at the same time, the four horizontal rudders are at the inertial working state. Assuming that the AUV is first pushed by waves to the left, it will roll to the right as shown in Fig. 5(b).The angular velocity sensor will transmit the roll information to controller, then the controller calculates the desired righting moment and drives the horizontal rudder to resist disturbance. Meantime, the horizontal rudder on the left side will rotate clockwise and generate lift along the negative direction of the Z-axis, the horizontal rudders on the right side will rotate clockwise and generate lift along the positive direction of the Z-axis. After the roll angle reaches maximum, it will swing to the left, then the AUV will return to the initial equilibrium position, the horizontal rudder also returns to the initial equilibrium position as shown in Fig. 5(c).Then the AUV is pushed by waves to the right, it will continue swing to the left, the horizontal rudders in left side will rotate anticlockwise and generate lift along the positive direction about Z-axis, the horizontal rudder in right side will rotate anticlockwise and generate lift along the negative direction of the Z-axis as shown in Fig. 5(d), when the roll angle reaches maximum, it will swing to the right. The AUV will return to its equilibrium position for the second time as shown in Fig. 5(e).With this, the AUV completes a period of roll reduction.

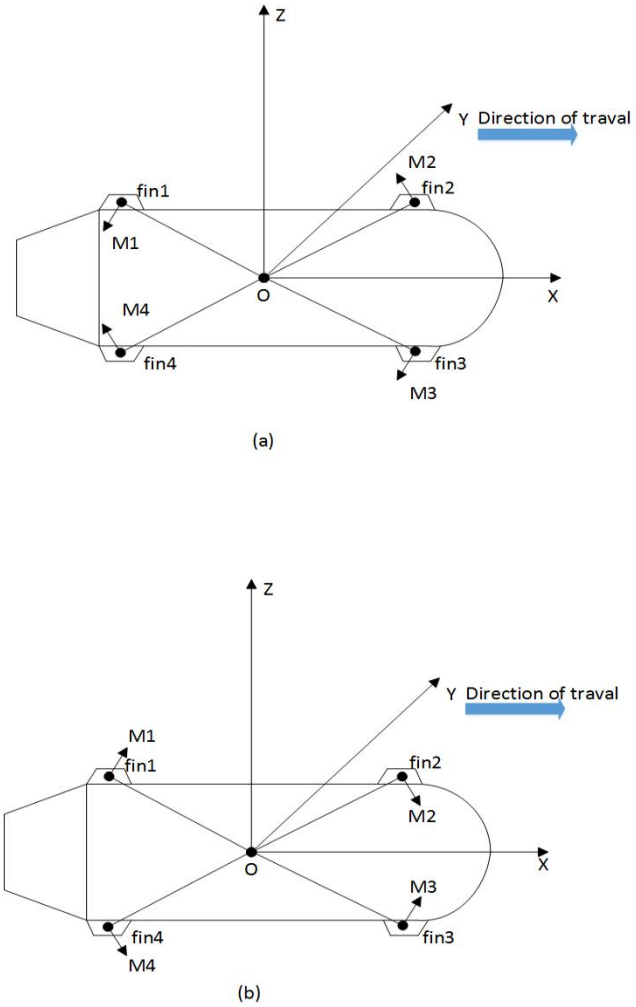

Fig. 6 Moment analysis

The above process is the roll stabilization of the underwater vehicle with horizontal rudders. When the AUV rolls to the right, moments of each lift relative to its centroid on horizontal rudders are shown in Fig. 6(a), and when the AUV rolls to the left, moments of lifts relative to its centroid on horizontal rudders are shown in Fig. 6(b). Through the analysis from two diagrams, moments direction of fin1 and fin3 is always the same, and the moments direction of fin2 and fin4 is always the same. In other words, fin1 and fin3 have the same stabilized effect to the AUV, and fin2 and fin4 have the same stabilized effect to the AUV. In order to realize the integrated control to reduce roll and pitch, and reduce the complexity of control system.

Assuming that the fin1 and fin3 rotate at the same speed, the fin2 and fin4 rotate at the same speed, the direction of rotation of fin1 and fin2 is same, and the direction of rotation of fin3 and fin4 is the same. If the velocity and acceleration of the fin1 and fin3 is ω_1 and $\dot{\omega}_1$ respectively, and the velocity and acceleration of the fin2 and fin3 is ω_2, $\dot{\omega}_2$ respectively, lifts on the fin1 and fin3 can be expressed as follows:

$$F_1(t) = \left(a_1\omega_1^2(t) + a_2\dot{\omega}_1(t)\right)\cos(\omega_1 t) \tag{19}$$

Where l_f is the roll righting arm; L_f is the pitch righting arm; and the moment of the lift $F_1(t)$ relatived to the roll axis can be expressed as follows:

$$M_{x1} = 2F_1(t)l_f = 2\left(a_1\omega_1^2(t) + a_2\dot{\omega}_1(t)\right)\cos(\omega_1 t)l_f \tag{20}$$

The moment of the lift $F_1(t)$ relatived to the pitch axis can be expressed as follows:

$$M_{y1} = 2F_1(t)L_f = 2\left(a_1\omega_1^2(t) + a_2\dot{\omega}_1(t)\right)\cos(\omega_1 t)L_f \tag{21}$$

Lifts on the fin2 and fin4 can be expressed as follows:

$$F_2(t) = \left(a_1\omega_2^2(t) + a_2\dot{\omega}_2(t)\right)\cos(\omega_2 t) \tag{22}$$

The moment of the lift $F_2(t)$ relatived to the roll axis can be expressed as follows:

$$M_{x2} = 2F_2(t)l_f = 2\left(a_1\omega_2^2(t) + a_2\dot{\omega}_2(t)\right)\cos(\omega_2 t)l_f \tag{23}$$

The moment of the lift $F_2(t)$ relatived to the pitch axis can be expressed as follows:

$$M_{y2} = -2F_2(t)L_f = -2\left(a_1\omega_2^2(t) + a_2\dot{\omega}_2(t)\right)\cos(\omega_2 t)L_f \tag{24}$$

In summary, the rolling righting moment of the AUV can be expressed as follows:

$$M_{fin1} = M_{x1} + M_{x2} = 2\left(a_1\omega_1^2(t) + a_2\dot{\omega}_1(t)\right)\cos(\omega_1 t)l_f + 2\left(a_1\omega_2^2(t) + a_2\dot{\omega}_2(t)\right)\cos(\omega_2 t)l_f \quad (25)$$

The pitching righting moment of the AUV can be expressed as follows:

$$M_{fin2} = M_{y1} + M_{y2} = 2\left(a_1\omega_1^2(t) + a_2\dot{\omega}_1(t)\right)\cos(\omega_1 t)L_f - 2\left(a_1\omega_2^2(t) + a_2\dot{\omega}_2(t)\right)\cos(\omega_2 t)L_f \quad (26)$$

Obviously, if fin1, fin2, fin3, and fin4 rotate at the same angular velocity and angular acceleration, namely, $\omega_1 = \omega_2$, $\dot{\omega}_1 = \dot{\omega}_2$, the integrated controller can not reduce pitch of the AUV, in other words, the integrated controller is the same as the roll reduction controller.

5.Control system for roll and pitch reduction

Motions of the underwater vehicle near the surface are coupled and nonlinear. The horizontal rudder based on the operating principle of zero speed fin stabilizer is used to stabilize the AUV. Based on the 6-DOF coupled and nonlinear model of the AUV and the hydrodynamic model of horizontal rudder, a modified sliding mode controller is designed to realize the integrated control of the roll and pitch of the AUV. The sliding mode control has many advantages, such as fast response speed, the controller is invariant to the parameter perturbation and the external disturbance of the controlled system, and easy physical realization, which is very suitable for the nonlinear time-varying system of the underwater vehicles. The sliding mode control includes of two processes: the approach motion and the sliding mode motion. The motion of the system from any initial state to the switching surface is called the approach motion. The ability of the sliding mode control only guarantees the system from any initial state to the switching surface in a finite time, and there is unrestricted tracks of the approach motion. The dynamic quality of the approach motion can be

improved by applying reaching law sliding mode control. Reaching law sliding mode control is a typical sliding mode control (Liu, 2015), and can be expressed as follows:

$$\dot{s} = -\varepsilon \operatorname{sgn} s - ks \tag{28}$$

Where ε is the velocity of the approach motion; k is a constant, $\varepsilon > 0, k > 0$ .The exponential reaching law sliding mode control can reduce the time to reach switching surface of system's state variables, and the speed of the reaching switching surface is very rapid, and making the dynamic quality of approach motion is better. However, the method cannot make system's state variables approach origin in the switching surface, and system's state variables chattering near the origin in the switching surface. Huang et al. (2013) presented a modified exponential reaching law sliding mode control is applied and the form of the expression is as follows:

$$\dot{s} = -\varepsilon e^{-\alpha t} s^{\beta} \operatorname{sgn} s - ks \tag{29}$$

Where ε is the reach law of sliding mode; k, α, β is constant, $\varepsilon > 0, k > 0, \alpha > 0, \beta > 0$; $e^{-\alpha t}$ is termed the fading factor. The modified exponential reaching law sliding mode control is brought the fading factor to make the system's state variables approach origin in the switching surface and eliminate the chattering of sliding motion control.

In order to eliminate chattering of the sliding mode control more efficiently, an adaptive neuron sliding mode is applied to adjust the reach law of the sliding mode ε in time (Pan, 2010; Wang, 1998; Wang, 2005). The adaptive neuron control algorithm is expressed as:

$$\begin{cases} \varepsilon(k) = k'\sum_{i=1}^{3} w_i'(k)x_i(k) + \varepsilon(k-1) \\ w_i'(k) = w_i(k) / \sum_{i=1}^{3} |w_i(k)| \\ w_i(k) = w_i(k-1) + \eta r_i(t) = w_i(k-1) + \eta e(k)s(k)x_i(k) \end{cases} \tag{30}$$

Where η is the learning speed, $\eta > 0$; $W_i(k)$ is the neuron weight; and k' is the coefficient of the neuron gain, k is the current time.

If:

$$e(k) = r_d(k) - s(k) \tag{31}$$

Where $r_d(k)$ is the ideal objective function; $s(k)$ is the actual switching function. The input of the neuron is defined as:

$$\begin{cases} x_1(k) = e(k) \\ x_2(k) = e(k) - e(k-1) \\ x_3(k) = e(k) - 2e(k-1) + e(k-2) \end{cases} \tag{32}$$

$w_i(k)$ establishes the supervised Hebb learning algorithm and it is expressed as:

$$r_i(k) = e(k)s(k)x_i(k) \tag{33}$$

For the roll motion equation, if $\dot{\phi}$ is set as p, namely, $\dot{\phi} = p$, and considering the rolling disturbance torque of waves and the rolling righting moment of the horizontal rudder, the roll motion equation is expressed as follows:

$$\begin{aligned} &(I_x - \frac{\rho}{2}L^5 K_{\dot{p}}')\ddot{\phi} = \\ &\frac{\rho}{2}L^5 K_{\dot{r}}'\dot{r} + \frac{\rho}{2}L^4(K_{\dot{v}}'\dot{v} + K_p'u\dot{\phi} + K_r'ur) + \frac{\rho}{2}L^3 K_v'uv - Z_G W\phi + M_{wx} + M_{fin1} \end{aligned} \tag{34}$$

If the ideal rolling angle ϕ_d is set as 0, namely, $\phi_d = 0$, the expression of the roll angular deviation e_{roll} is given by:

$$\begin{cases} e_{roll}(t) = \phi_d - \phi(t) = -\phi(t) \\ \dot{e}_{roll}(t) = \dot{\phi}_d - \dot{\phi}(t) = -\dot{\phi}(t) \\ \ddot{e}_{roll}(t) = \ddot{\phi}_d - \ddot{\phi}(t) = -\ddot{\phi}(t) \end{cases} \tag{35}$$

The actual rolling sliding mode switching surface is expressed as:

$$s_1 = \dot{e}_{roll} + C_{roll} e_{roll} = -\dot{\phi}(t) - C_{roll}\phi(t) \tag{36}$$

The modified exponential reaching law sliding mode control for the roll motion is expressed as:

$$\dot{s}_1 = -\varepsilon_1 e^{-\alpha_1 t} s_1^{\beta_1} \operatorname{sgn} s_1 - k_1 s_1 \tag{37}$$

Where ε_1 is the reach law of sliding mode; k_1, α_1, β_1 are constant, $\varepsilon_1 > 0,\ k_1 > 0,\ \alpha_1 > 0,\ \beta_1 > 0$ .The derivative of equation is expressed as:

$$\dot{s}_1(t) = -\ddot{\phi}(t) - C_{roll}\dot{\phi}(t) \tag{38}$$

By combining Eq.(37) and Eq.(38), the expression for $\ddot{\phi}$ is given by

$$\ddot{\phi}(t) = \varepsilon_1 e^{-\alpha_1 t} s_1^{\beta_1} \operatorname{sgn} s_1 + k_1 s_1 - C_{roll}\dot{\phi}(t) \tag{39}$$

By combining Eq.(34) and Eq.(39), the roll motion equation is expressed as:

$$\begin{aligned} &(I_x - \frac{\rho}{2}L^5 K'_{\dot{p}})(\varepsilon_1 e^{-\alpha_1 t} s_1^{\beta_1} \operatorname{sgn} s_1 + k_1 s_1 - C_{roll}\dot{\phi}(t)) - \frac{\rho}{2}L^5 K'_{\dot{r}}\dot{r} - \frac{\rho}{2}L^4(K'_{\dot{v}}\dot{v} + K'_p u\dot{\phi} + K'_r ur) \\ &-\frac{\rho}{2}L^3 K_v' uv + Z_G W\phi - M_{wx} - M_{fin1} = 0 \end{aligned} \tag{40}$$

Similarly, for the pitch motion equation, where $\dot{\theta}$ is set q, namely, $\dot{\theta} = q$, and

392 considering the pitching disturbance torque of waves and the pitching righting
393 moment of horizontal rudder, the pitch motion equation is expressed as follows:

394 $$(I_y - \frac{\rho}{2}L^5 M'_{\dot{q}})\ddot{\theta}(t) = \frac{\rho}{2}L^4(M'_{\dot{w}}\dot{w} + M'_{uq}uq) + \frac{\rho}{2}L^3 M'_{uw}uw - Z_G w\sin\theta + M_{wy} + M_{fin2} \quad (41)$$

395 If the ideal pitching angle θ_d is set as 0, namely, $\theta_d = 0$, the expression for
396 pitching angular deviation e_{pitch} is given by:

397 $$\begin{cases} e_{pitch}(t) = \theta_d - \theta(t) = -\theta(t) \\ \dot{e}_{pitch}(t) = \dot{\theta}_d - \dot{\theta}(t) = -\dot{\theta}(t) \\ \ddot{e}_{pitch}(t) = \ddot{\theta}_d - \ddot{\theta}(t) = -\ddot{\theta}(t) \end{cases} \quad (42)$$

398 The actual pitching sliding mode switching surface is expressed as:

399 $$s_2 = \dot{e}_{pitch} + C_{pitch}e_{pitch} = -\dot{\theta}(t) - C_{pitch}\theta(t) \quad (43)$$

400 The modified exponential reaching law sliding mode control for pitch motion is
401 expressed as:

402 $$\dot{s}_2 = -\varepsilon_2 e^{-\alpha_2 t}s_2^{\beta_2}\operatorname{sgn}s_2 - k_2 s_2 \quad (44)$$

403 Where ε_2 is the reach law of sliding mode, k_2, α_2, β_2 are constant,
404 $\varepsilon_2 > 0$, $k_2 > 0$, $\alpha_2 > 0$, $\beta_2 > 0$. The derivative of equation is expressed as:

405 $$\dot{s}_2(t) = -\ddot{\theta}(t) - C_{pitch}\dot{\theta}(t) \quad (45)$$

406 By combining Eq.(44) and Eq.(45), the expression for $\dot{\theta}$ is given by

407 $$\ddot{\theta}(t) = \varepsilon_2 e^{-\alpha_2 t}s_2^{\beta_2}\operatorname{sgn}s_2 + k_2 s_2 - C_{pitch}\dot{\theta}(t) \quad (46)$$

408 By combining Eq.(40) and Eq.(46), the pitch motion equation is expression as:

$$(I_y - \frac{\rho}{2}L^5 M'_{\dot{q}})(\varepsilon_2 e^{-\alpha_2 t} s_2^{\beta_2} \operatorname{sgn} s_2 + k_2 s_2 - C_{pitch}\dot{\theta}(t)) - \frac{\rho}{2}L^4(M'_{\dot{w}}\dot{w} + M'_{uq}uq)$$
$$-\frac{\rho}{2}L^3 M'_{uw}uw + Z_G w\sin\theta - M_{wy} - M_{fin2} = 0 \tag{47}$$

The fin accelerations $\dot{\omega}_1$, $\dot{\omega}_2$ can be calculated from the roll motion equation and pitch motion equation. According to the approximate linearization method in small time interval, ω and α is calculated by:

$$\begin{cases} \omega_k = \omega_{k-1} + \dot{\omega}_{k-1}T \\ \alpha_k = \alpha_{k-1} + \omega_{k-1}T \end{cases} \tag{49}$$

Where α is the angle of the horizontal rudder; T is the sample time, set values of the sample time is 1ms, namely, $T = 1ms$; k is the current time.

6.Simulation Research

The simulation is based on the ITTC two-parameter wave spectrum and the significant wave height is 1m. The other relevant parameters are shown in TABLE I.

TABLE I

The relevant parameters of simulation research

The total length of the NPS AUV II	5.3m
The height of the NPS AUV II	0.5m
The width of the NPS AUV II	1m
The navigating depths of AUV	5m and 10m, respectively
Wave encounter angle	45°, 90°, and 135°, respectively
The navigating speed of AUV	1.832m/s
The ideal rolling angle	0
The ideal pitching angle	0
The chord length of the horizontal rudder	0.5m
The span length of the rudder	0.25m

The distance between the midpoint and the shaft of the rudder	0.125m
The rolling righting arm	0.625m
The pitching righting arm	2m
ε_1	0.04
α_1	0.1
β_1	2
k_1	0.6
ε_2	0.01
α_2	0.1
β_2	2
k_2	0.8
C_{roll}	0.3
C_{pitch}	0.3
k'	0.5
η	2

421 Simulation results is shown under different conditions as follows:

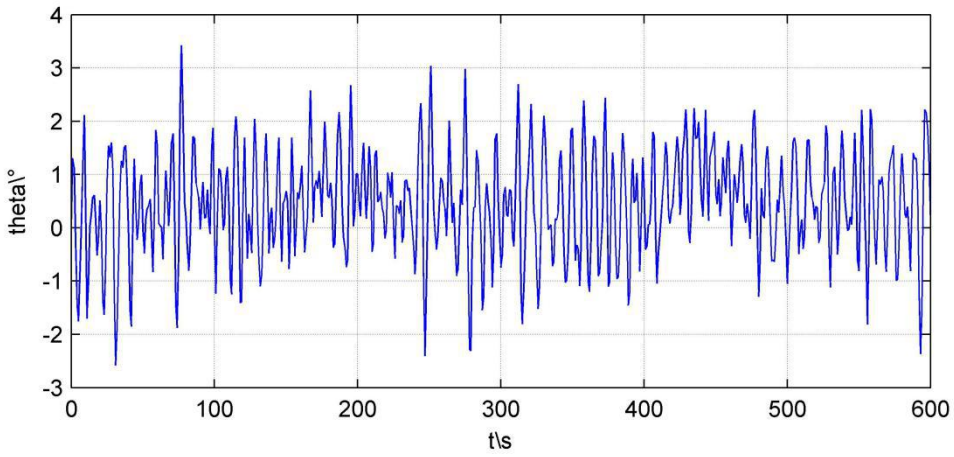

422

423 Fig.7 The pitch of the AUV without control when $h_B = 5m, \gamma = 45°$

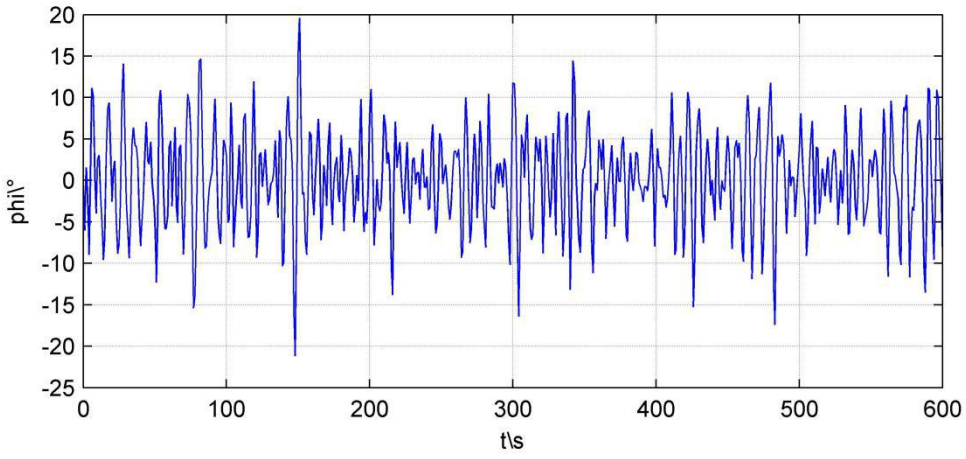

424

425 Fig.8 The roll of the AUV without control when $h_B = 5m, \gamma = 45°$

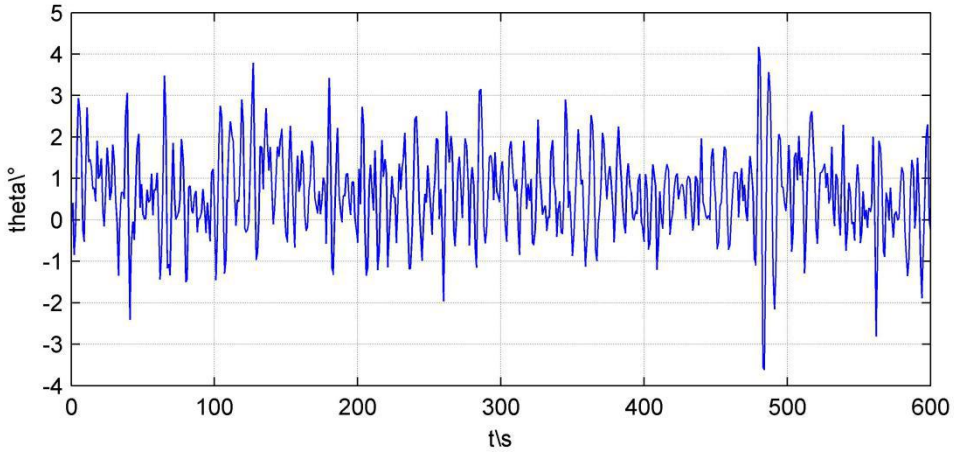

426

427 Fig.9 The pitch of the AUV without control when $h_B = 5m, \gamma = 90°$

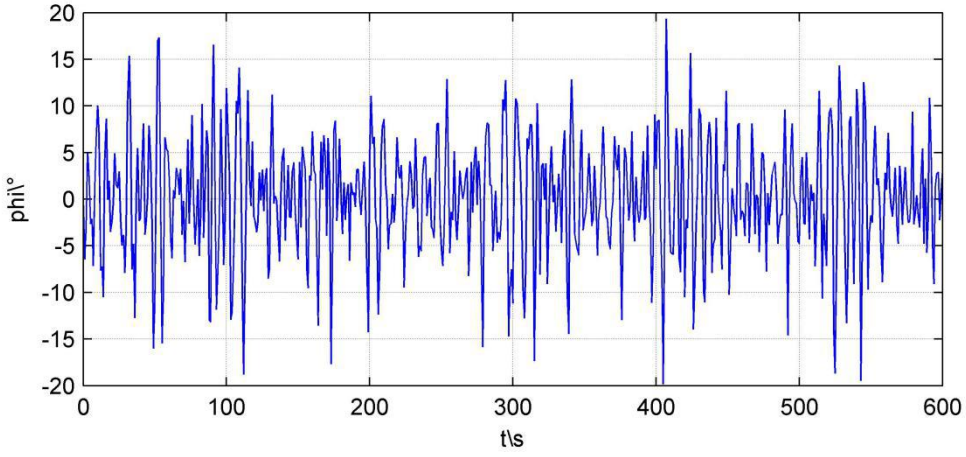

428

429 Fig.10 The roll of the AUV without control when $h_B = 5m, \gamma = 90°$

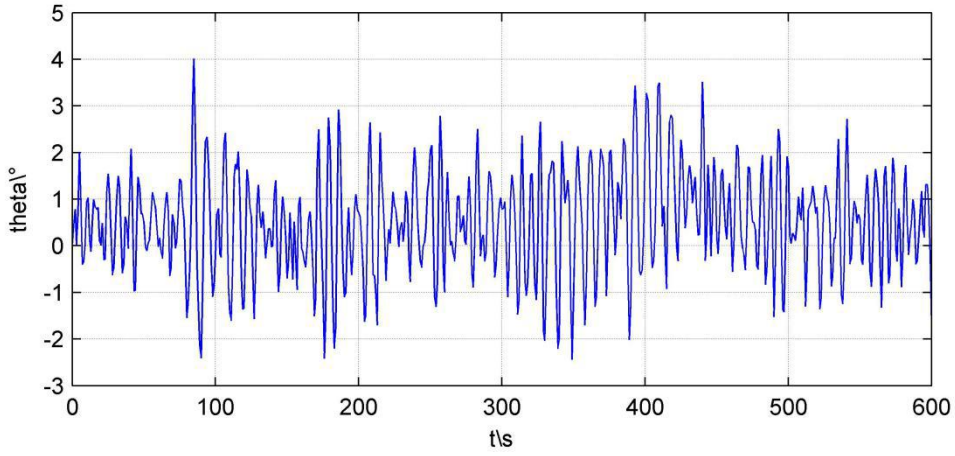

430

431 Fig.11 The pitch of the AUV without control when $h_B = 5m, \gamma = 135°$

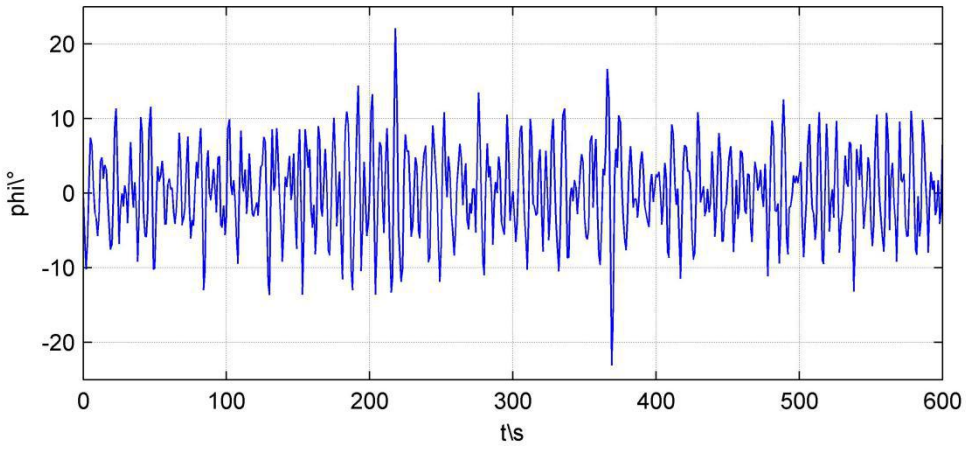

432

433 Fig.12 The roll of the AUV without control when $h_B = 5m, \gamma = 135°$

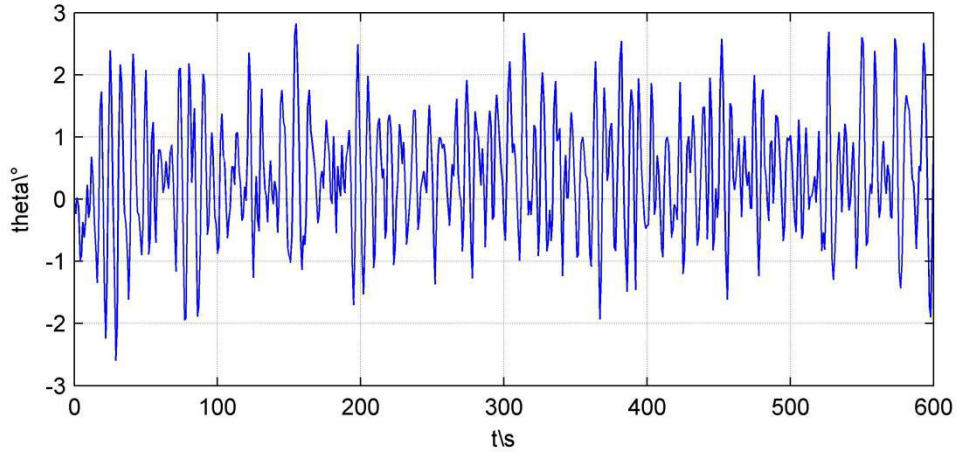

434

435 Fig.13 The pitch of the AUV without control when $h_B = 10m, \gamma = 45°$

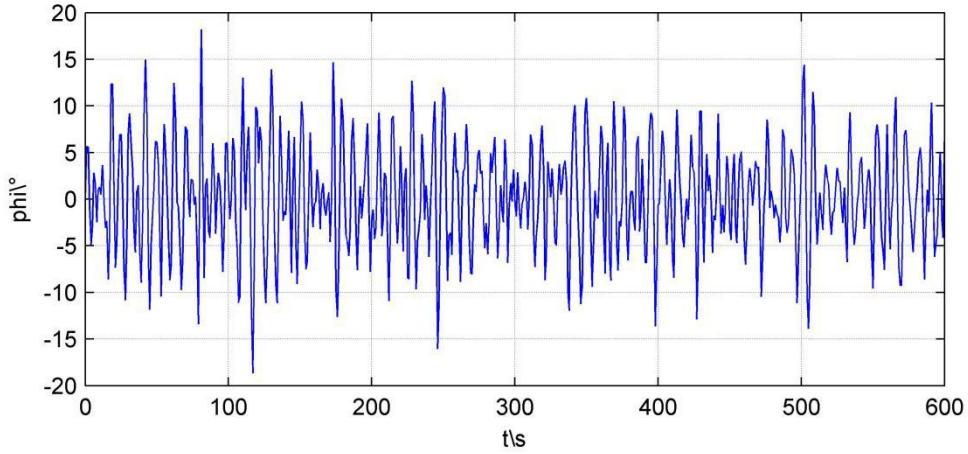

436

437 Fig.14 The roll of the AUV without control when $h_B = 10m, \gamma = 45°$

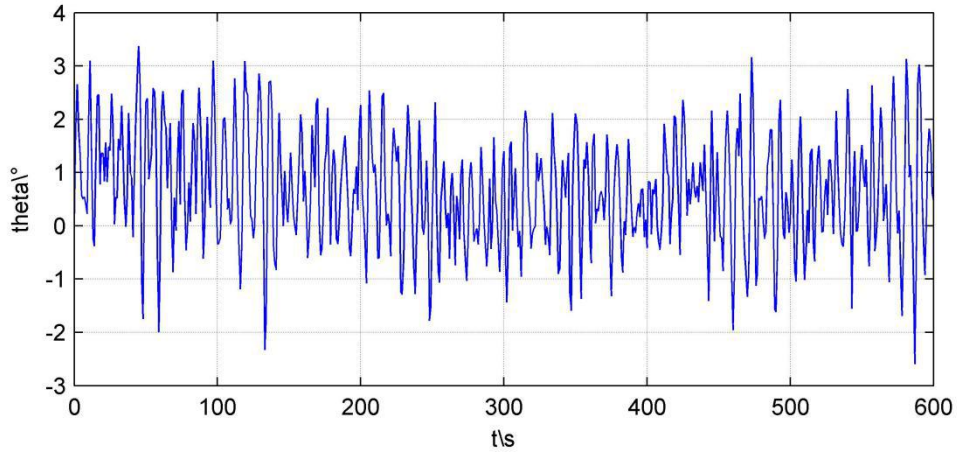

438

439 Fig.15 The pitch of the AUV without control when $h_B = 10m, \gamma = 90°$

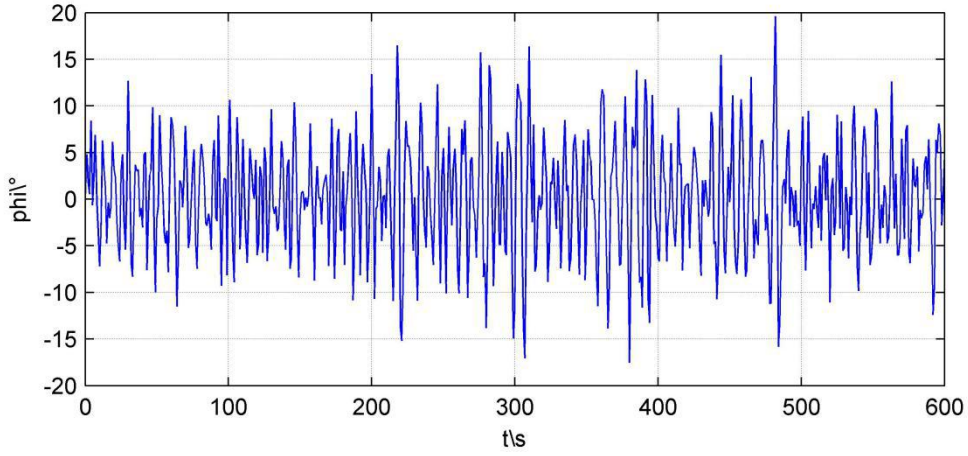

440

441 Fig.16 The roll of the AUV without control when $h_B = 10m, \gamma = 90°$

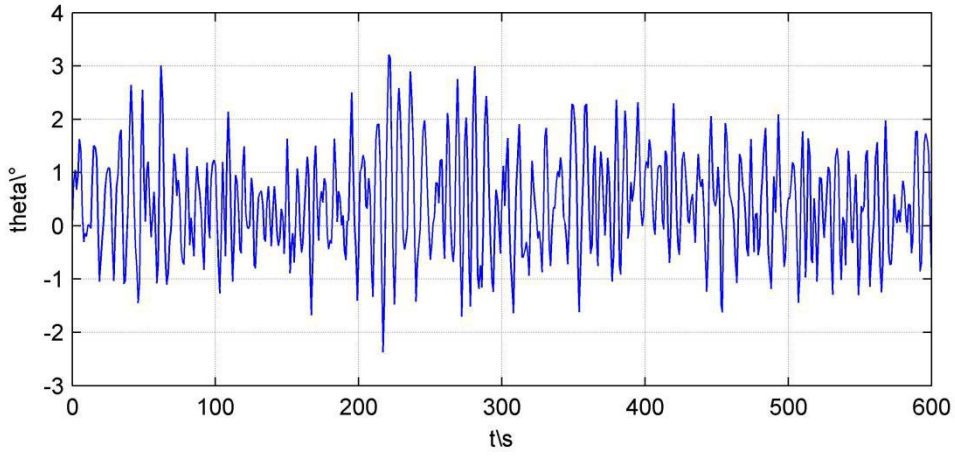

442

443 Fig.17 The pitch of the AUV without control when $h_B = 10m, \gamma = 135°$

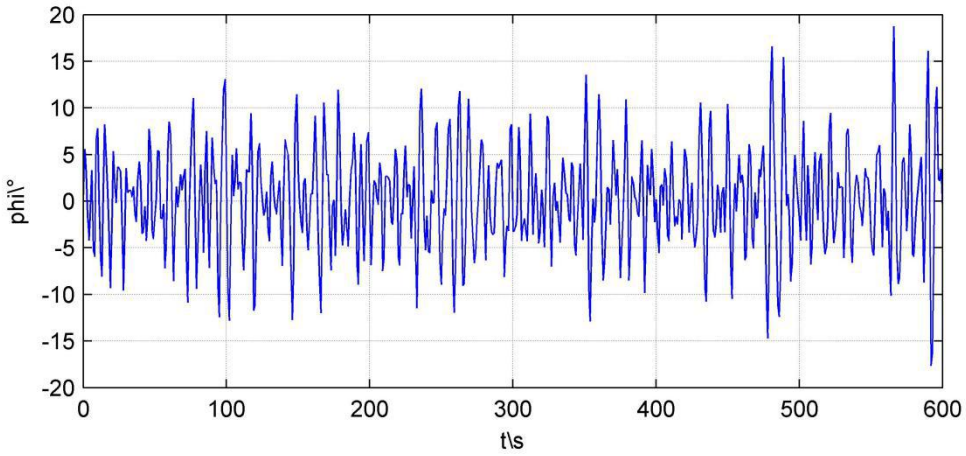

444

445 Fig.18 The roll of the AUV without control when $h_B = 10m, \gamma = 135°$

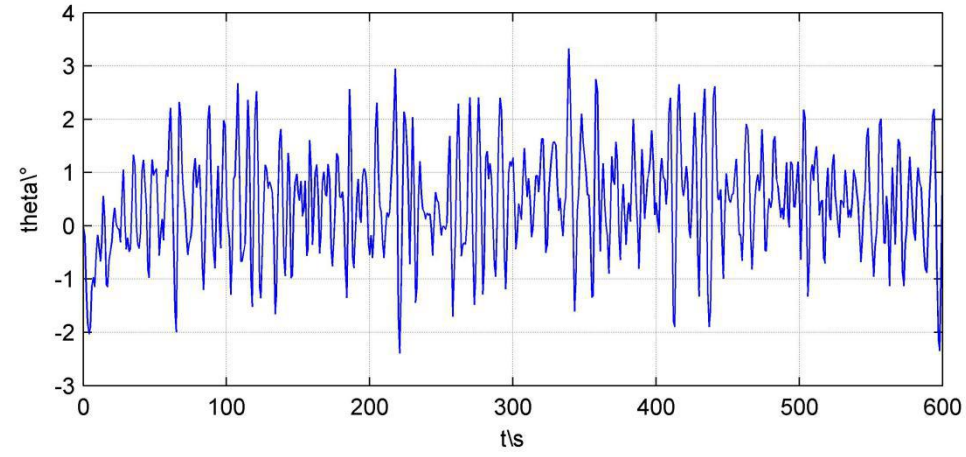

446

447 Fig.19 The pitch of the AUV with the roll reduction controller when $h_B = 5m, \gamma = 45°$

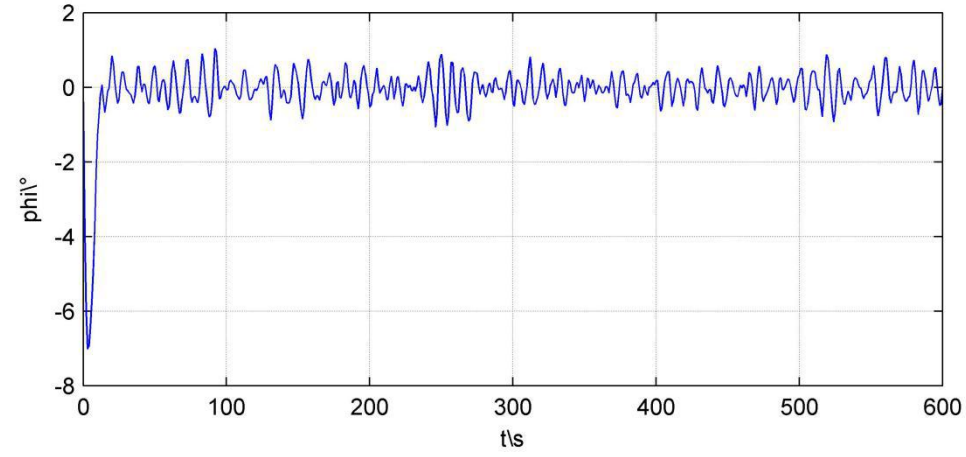

448

449 Fig.20 The roll of the AUV with the roll reduction controller when $h_B = 5m, \gamma = 45°$

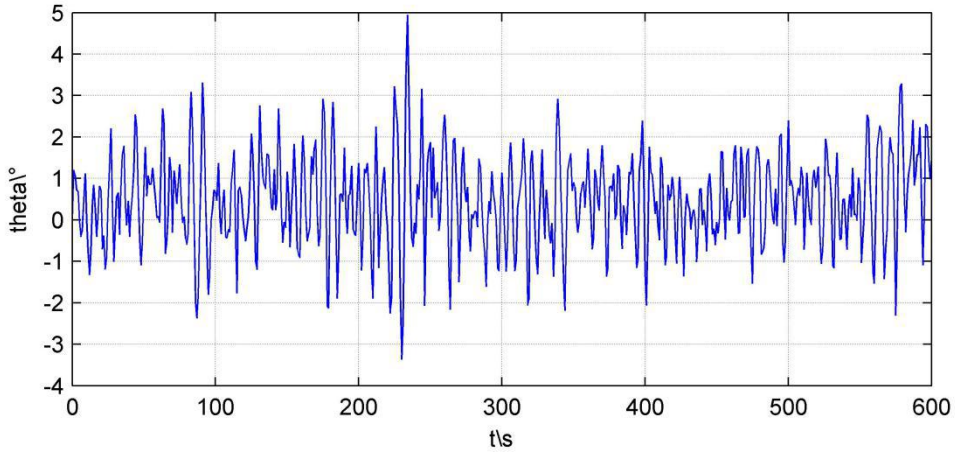

450

451 Fig.21 The pitch of the AUV with the roll reduction controller when $h_B = 5m, \gamma = 90°$

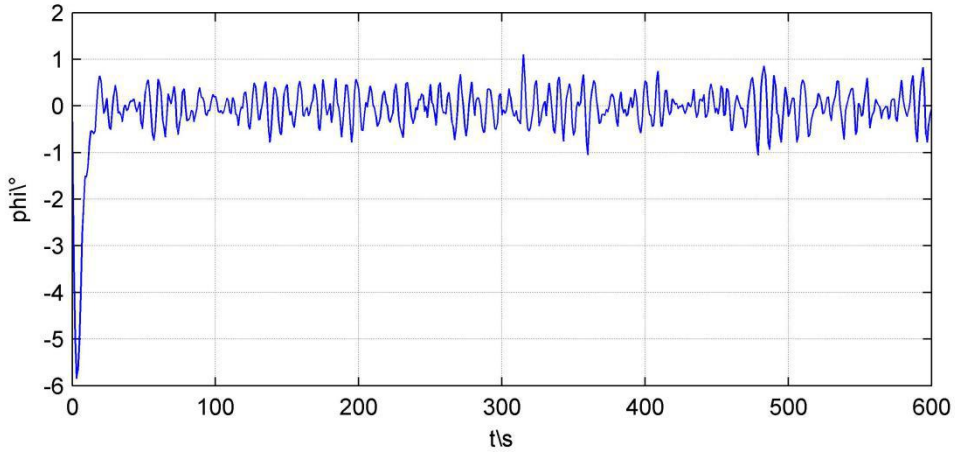

452

453 Fig.22 The roll of the AUV with the roll reduction controller when $h_B = 5m, \gamma = 90°$

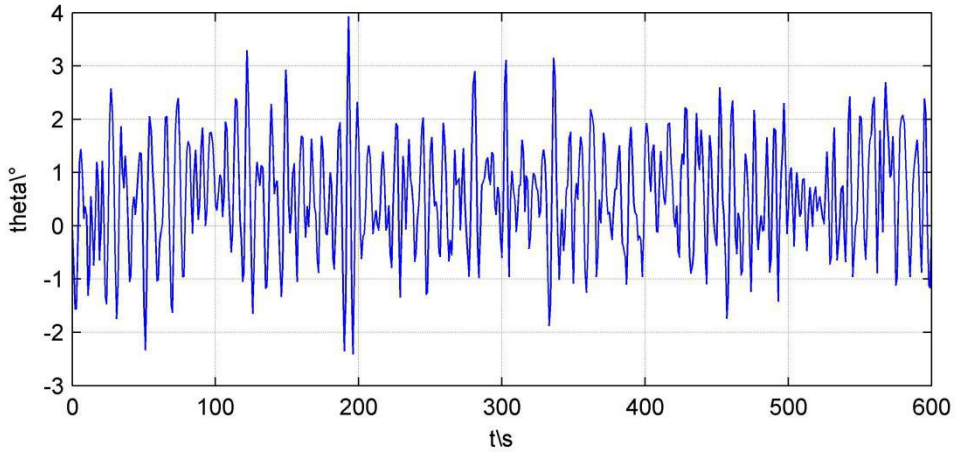

Fig.23 The pitch of the AUV with the roll reduction controller when

$$h_B = 5m, \gamma = 135°$$

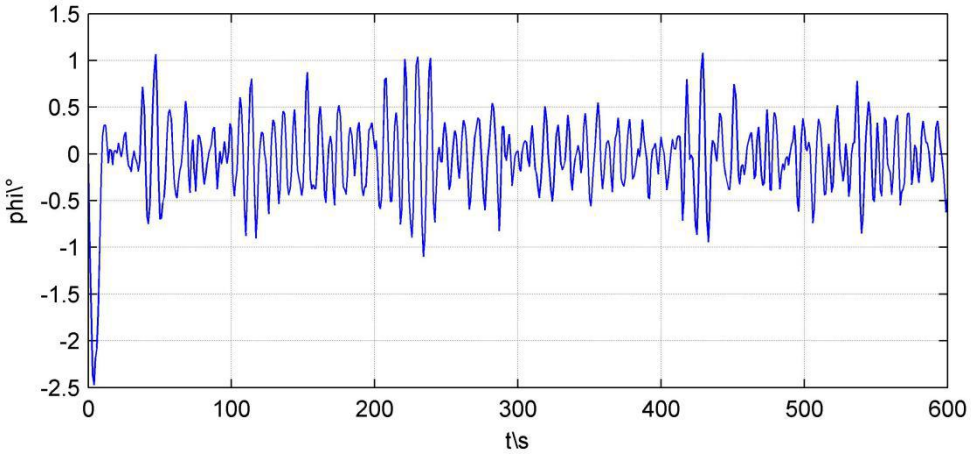

Fig.24 The roll of the AUV with the roll reduction controller when $h_B = 5m, \gamma = 135°$

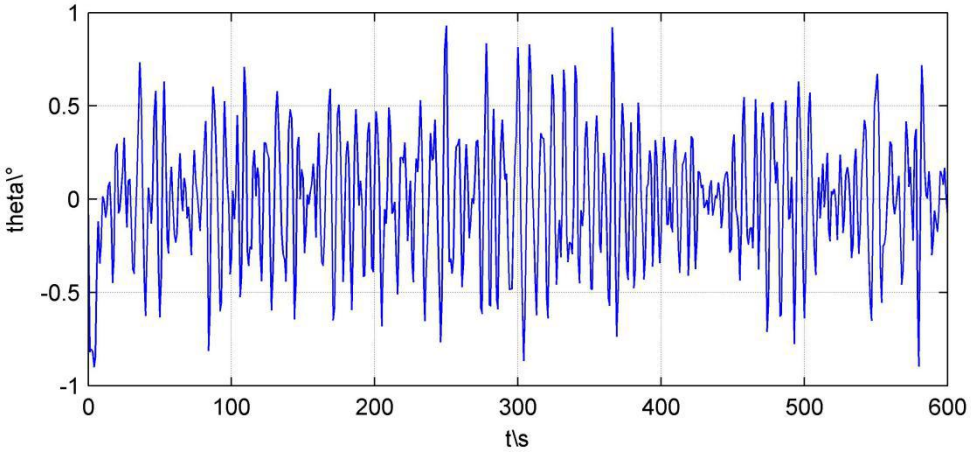

460 Fig.25 The pitch of the AUV with the integrated controller when $h_B = 5m, \gamma = 45°$

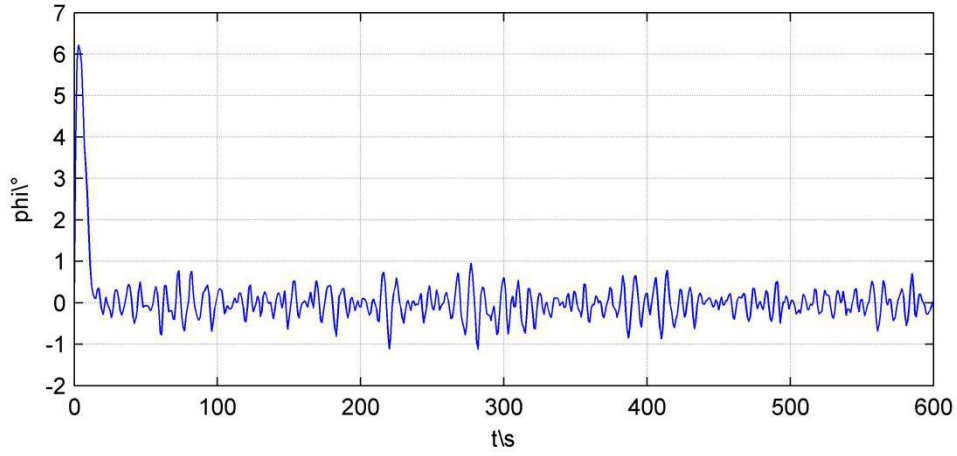

461

462 Fig.26 The roll of the AUV with the integrated controller when $h_B = 5m, \gamma = 45°$

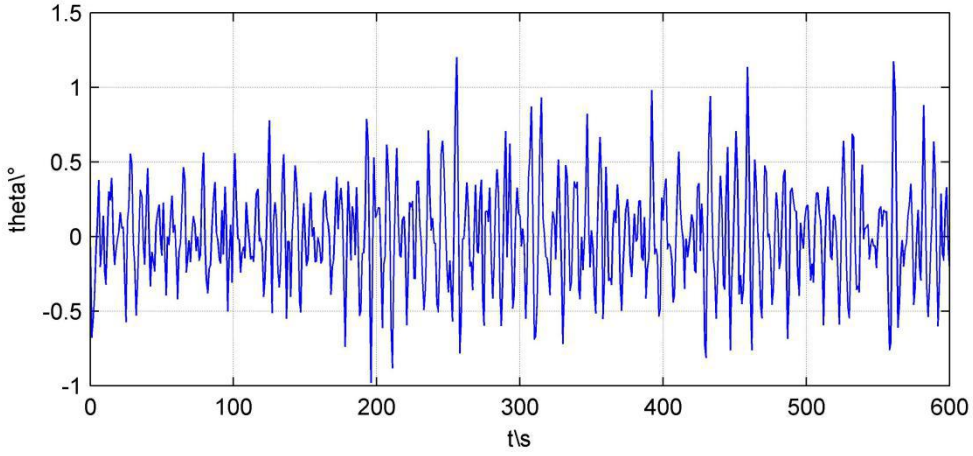

463

464 Fig.27 The pitch of the AUV with the integrated controller when $h_B = 5m, \gamma = 90°$

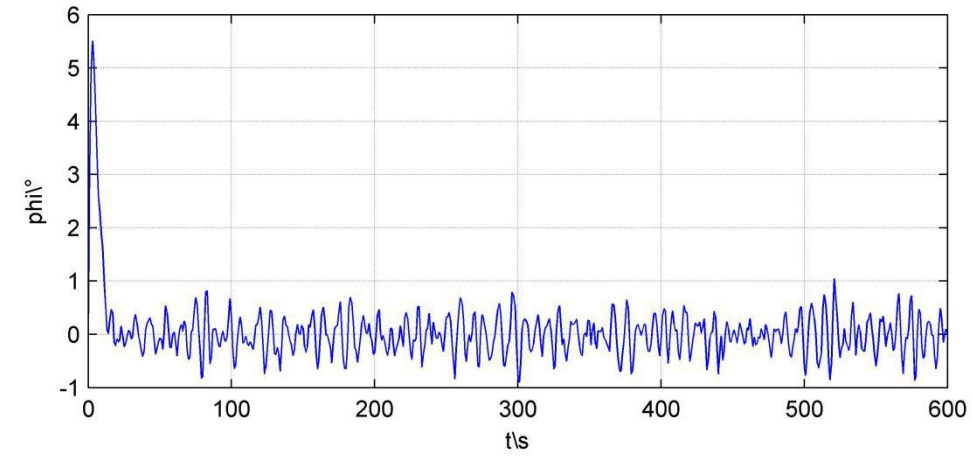

465

466 Fig.28 The roll of the AUV with the integrated controller when $h_B = 5m, \gamma = 90°$

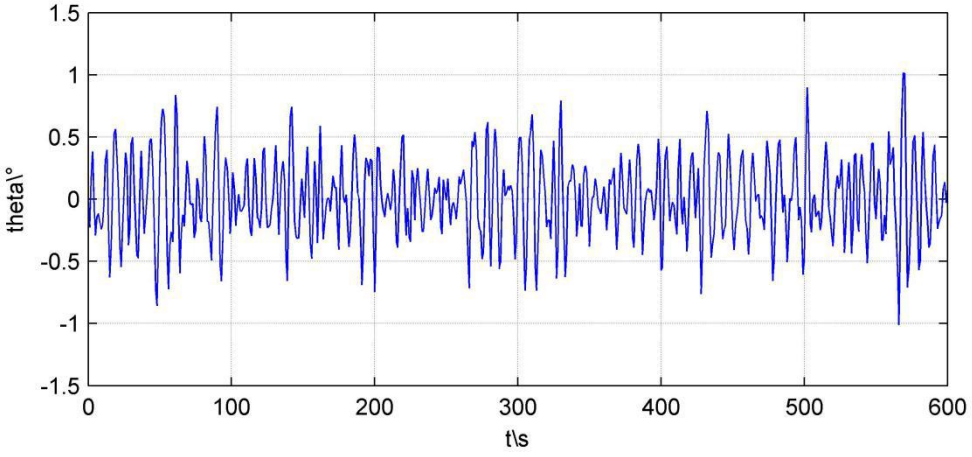

467

468 Fig.29 The pitch of the AUV with the integrated controller when $h_B = 5m, \gamma = 135°$

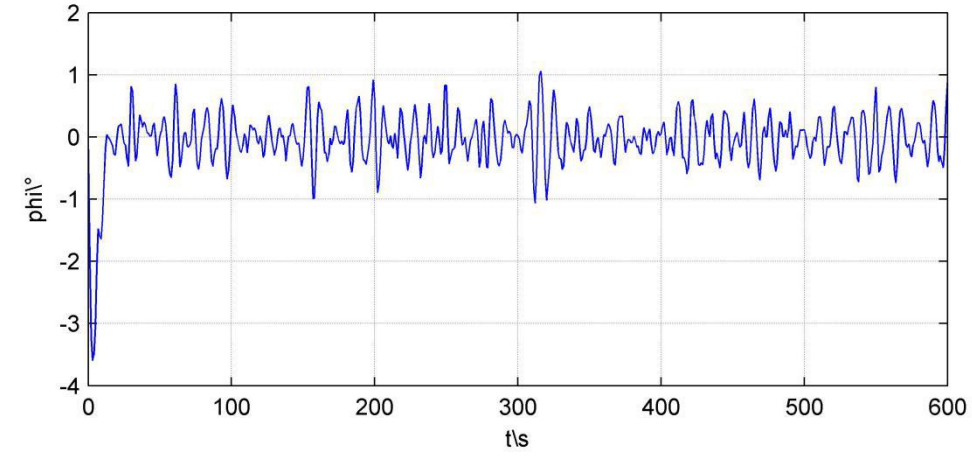

469

Fig.30 The roll of the AUV with the integrated controller when $h_B = 5m, \gamma = 135°$

Fig.8, 10, 12, 14, 16, 18 presents the results of the roll of the AUV without control. Fig.20, 22, 24 presents the results of the roll of the AUV under the control of the roll reduction controller. Fig.26, 28, 30 presents the results of the roll of the AUV under the integrated controller. Comparing these figures, it shows that the AUV with the horizontal rudder can reduce roll effectively.

Fig.7, 9, 11 presents results of the pitch of the AUV without control.Fig.25, 27, 29 presents results of the pitch of the AUV under the integrated controller. It can be seen that the AUV with horizontal rudder can also reduce pitch effectively. It indicates that the roll and pitch of the AUV is both reduced. So the AUV with the horizontal rudder can realized the integrated control of the roll and pitch motion of the AUV.

Stabilization efficiency is defined as follow:

$$stabilization\ efficiency = \frac{(roll(pitch)angle\ \mathrm{var}iance - (anti-roll(anti-pitch)angle\ \mathrm{var}iance))}{roll(pitch)angle\ \mathrm{var}iance}$$

Based on above definition, statistics of the roll stabilization and pitch stabilization of the AUV are shown in TABLE II and TABLE III respectively.

TABLE II

ROLL STABILIZATION EFFECT

Wave encounter angle /deg	Depth /m	Roll angle variance of vehicle without integrated controller /deg	Roll angle variance of vehicle with roll reduction	Roll stabilization effect of vehicle with roll	Roll angle variance of vehicle without integrated controller /deg	Roll stabilization effect of vehicle with integrated controller /%

			controller /deg	reduction controller /%		
45°	5m	32.28	0.34	98.94	0.46	98.67
	10m	30.30	0.27	99.11	0.40	98.68
90°	5m	38.87	0.71	98.17	0.76	98.04
	10m	35.21	0.66	98.13	0.65	98.15
135°	5m	32.97	0.37	98.88	0.43	98.70
	10m	29.98	0.26	99.13	0.40	98.67

TABLE III

PITCH STABILIZATION EFFECT

Wave encounter angle /deg	Depth /m	Pitch angle variance of vehicle without integrated controller /deg	Pitch angle variance of vehicle with roll reduction controller /deg	Pitch angle variance of vehicle without integrated controller /deg	Pitch stabilization effect of vehicle with integrated controller /%
45°	5m	1.06	1.09	0.10	90.57
	10m	0.99	1.00	0.11	88.89
90°	5m	1.17	1.15	0.11	82.05
	10m	1.05	1.07	0.10	90.48
135°	5m	0.92	1.05	0.10	89.13
	10m	0.89	0.95	0.09	89.89

From TABLE II, it can be seen that the roll stabilization efficiency in different simulation conditions is over 98％, which indicates using the horizontal rudder to

reduce the roll motion of the AUV is effective.

From TABLE III, it can be seen that the pitch stabilization efficiency in different simulation conditions is also good, and is over 80%.

Thus, so the underwater vehicle can reduce the roll and pitch effectively by using the horizontal rudder.

7.Conclusion

In this paper, a new method to reduce the roll and pitch of the AUV is presented and designed. The horizontal rudder using the lift principle of zero speed fin stabilizer is shown to reduce the roll and pitch of the underwater vehicle. Basing on the underwater vehicle's 6-DOF nonlinear and coupling motions, the hydrodynamic model of horizontal rudder, and wave disturbance model, a modified sliding mode integrated controller is designed to reduce the roll and pitch under different wave disturbances. From these simulations, it shows that the control law can reduce the roll and pitch of the underwater vehicle effectively.

REFERENCES

Yan, Z.P., Zhou, J.J, 2015. Underwater unmanned vehicle control technology. National Defense Industry Press, Beijing.

Qi, Z., Jin, H., Zhou, A., Pang, Y., 2011. Research on a method to reduce roll and pitch of AUV based on active bionic fin stabilizer. Control and Decision Conference (pp.2778-2782). IEEE.

Qi, Z., Jin, H., Meng, L., Pang, Y., 2011. Research on a fuzzy immune PID controller to reduce roll of near-water-surface vehicle with active bionic fin stabilizer.

International Conference on Intelligent Control and Information Processing (Vol.1, pp.82-86). IEEE.

Fang, M.C., Chang, P.E., Luo, J.H., 2006. Wave effects on ascending and descending motions of the autonomous underwater vehicle. Ocean Engineering, 33(14–15), 1972-1999.

Mills, D., Harris, C. J., 1995. Neurofuzzy modelling and control of a six degree of freedom auv.

Petrich, J., Stilwell, D. J., 2010. Model simplification for AUV pitch-axis control design. Ocean Engineering, 37(7), 638-651.

Fan, W., Jin, H., Qi, Z., 2009. Modeling for active fin stabilizers at zero speed. Ocean Engineering, 36(17), 1425-1437.

Jin, H., Z., Zhang, X.F., Luo, Y.M., Li, D.S., 2007. Research on lift model of zero speed fin stabilizer. China Ocean Engineering, 25(3), 83-87.

Qi., 2008. Research on the lift mechanism and the system model of fin stabilizer at zero speed. PhD thesis, Harbin Engineering University, Harbin, 78-95.

Cui, R., Zhang, X., Cui, D., 2016. Adaptive sliding-mode attitude control for autonomous underwater vehicles with input nonlinearities. Ocean Engineering, 123, 45-54.

Jantapremjit, P., Wilson, P., 2007. Optimal control and guidance of homing and docking tasks using an autonomous underwater vehicle. 243-248.

Hao, Y., Zhao, X., 2013. Slide-mode variable-structure AUV attitude control on the basis of fuzzy switching. Caai Transactions on Intelligent Systems, 8(6), 532-536.

539 Jafarov, E.M., asaltin, R., 2000. Robust sliding-mode control for the uncertain mimo
540 aircraft model f-18. IEEE Transactions on Aerospace & Electronic Systems,
541 36(4), 1127-1141.

542 Rhif, A., Kardous, Z., Braiek, N. B. H., 2011. A high order sliding mode-multimodel
543 control of nonlinear systems simulation on a submarine mobile. International
544 Multi-Conference on Systems, Signals and Devices (pp.1-6). IEEE.

545 Jantapremjit, P., Wilson, P. A., Murphy, A. J., 2006. A study of autonomous docking
546 with an AUV using intelligent controls. *International conference on Underwater*
547 *System Technology: Theory and Applications*(pp.12-16)

548 Warner, D. C., 1991. Design, simulation, and experimental verification of a computer
549 model and enhanced position estimator for the NPS AUV II. Monterey California
550 NavalPostgraduate School.

551 Healey, A.J., Marco, D.B., 1992. Experimental verification of mission planning by
552 autonomous mission execution and data visualization using the NPS AUV II.

553 Fossen, T.I., 1994. Guidance and Control of Ocean Vehicles, Wiley, Chichester.

554 Jin, H.Z., Yao, X.l.(2001).Ship Control Theory.Harbin: Harbin Engineering University
555 Press, ch 2, 3, 4.

556 Ji, X.M., 2009. Research on synthetic anti-rolling technology of small submersible
557 based on bionic wing. Master thesis, Harbin Engineering University, Harbin.

558 Jin, H. Z., Yu, W., Qi, Z. G., Jin, G., 2007. Study on Lift Generation of Weis-Fogh
559 Flapped Fin Stabilizer at Zero Speed. *SICE-ICASE, 2006. International Joint*
560 *Conference* (pp.1521-1524). IEEE.

561 Liu, J.K., 2015. MATLAB Simulation of sliding Mode variable structure Control.
562 Tsinghua University Press.

563 Huang, H., Li, G., Liu, L.H., Lin, P., 2013. Research of a Sliding Mode Control
564 Strategy for Manipulator Arm Based on Reaching Law. Journal of Hunan
565 University of Technology, 27(1), 62-66.

566 Pan, L.X., 2010. Research on Control Strategy of AUV Roll Stabilizing near Surface.
567 PhD thesis, Harbin Engineering University, Harbin.

568 Wang, Y.J., 1998. Neural network control. China Machine Press.

569 Wang, S.Y., 2005. Intelligent control system and application. China Machine Press.